Electrical, optical and structural properties of transparent and conducting ZnO thin films doped with Al and F by rf magnetron sputter

B.G. Choi[1)], I.H. Kim[*], D.H Choi[1)], K.S. Lee, T.S. Lee, B. Cheong,

Y.-J. Baik, and W.M. Kim

Thin Film Materials Research Center, Korea Institute of Science and Technology, 39-1, Hawolgok-dong, Sungbuk-gu, Seoul 136-791, Korea

1) Division of Materials Science and Engineering, Korea University Anam-Dong 5-1, Sungbuk-gu, Seoul 136-701, Korea

*e-mail : inhok@kist.re.kr

Abstract

Al and F-doped ZnO films were prepared on glass substrates by co-sputtering ZnO targets composed of 2 wt % Al_2O_3, 1.3 wt % ZnF_2 and pure ZnO targets respectively. The resistivity of as-deposited ZnO films at room temperature was in the range of $2.3\times10^{-3} \sim 7.0\times10^{-4}$ Ωcm with Al and F contents in the films. After annealing in vacuum pressure of 10^{-6} Torr at 300 ºC for 2 h, the resistivity of ZnO films decreased down to 4.7×10^{-4} Ωcm and ZnO film which composed of Al-doped ZnO 25 % and F-doped ZnO 75 % by volume fraction showed the highest mobility of 42.2 cm^2/Vsec. From XRD measurements it was found that F dopants promote crystallization of ZnO films. Form XPS spectra of oxygen 1s binding energy and Hall measurements it was confirmed that by vacuum annealing chemisorbed oxygens at the grain boundary desorbed and reduced grain boundary scattering. Also figure of merit (FOM) defined as ratio of the electrical conductivity to the optical absorption coefficient increased up to 2.67 Ω^{-1} after post annealing.

Keywords : Electrical properties, ZnO, Transparent and conducting oxide

1. Introduction

ZnO thin films doped with Al, Ga or In have low electrical resistivity and high optical transmittance due to their high carrier concentrations above 10^{20} cm^{-3} and wide optical band gap energy of above 3.3 eV [1]. Recently, Al doped ZnO thin films (AZO) have drawn a great deal of attention due to their low material cost, non-toxicity and the stability under the hydrogen plasma compared to ITO (Sn doped indium oxide) [2]. Most of the studies on doped ZnO thin films were carried out using trivalent cation dopants such as Al, Ga and B [3]. However, only a few studies on fluorine doped ZnO (FZO) can be found in the literature despite the fact that fluorine can be an adequate anion doping candidate due to its similar ionic radius to oxygen. Most of the studies on FZO thin films were made using chemical process of sol-gel or spray pyrolysis [4-6], and the resistivity of FZO prepared by spray pyrolysis was in the range of $10^{-1} \sim 10^{-2}$ Ωcm [6]. The most notable result were obtained for FZO thin films deposited using CVD technique by Hu and Gordon, in which the resistivity as low as of 4×10^{-4} Ωcm and high mobility as high as 40 cm^2/Vsec were reported [7]. The low resistivity combined with high mobility of FZO film was attributed to the restricted perturbation effect of fluorine anion to valence band [7]. Unlike metallic dopants, however, fluorine is known to be difficult to be incorporated into ZnO films by PVD technique like sputtering [8].

In this study, to make advantage of Al dopants which can be easily incorporated into Zn sites and F dopants which can not be easily incorporated but give high mobility, Al and F dually doped ZnO films (AFZO) were prepared by co-sputtering of ZnO target containing Al_2O_3 (AZO) and ZnO target containing ZnF_2 (FZO), and their electrical, optical and structural

properties were investigated.

2. Experimental Details

AZO, FZO and AFZO thin films were deposited on corning glass substrates (Eagle 2000) by rf magnetron sputtering with 2" diameter targets. $ZnO:Al_2O_3$ (AZO) and $ZnO:ZnF_2$ (FZO) targets contained 2 wt% Al_2O_3 and 1.3 wt% ZnF_2, respectively. By varying the rf power applied on each target during co-sputtering, ZnO films with five different chemical compositions were prepared (AFZO series). The volume ratios of FZO to AZO in AFZO film series were 1:0, 3:1, 1:1, 1:3, and 0:1, and the corresponding AZO volume fraction was 0, 25, 50, 75 and 100 %, respectively. The applied rf power on FZO and AZO target is 50 and 0 W for 1:0 of FZO to AZO volume ratio (FZO), 50 and 24 W for 3:1 (AFZO25), 50 and 50 W for 1:1 (AFZO50), 24 and 50 W for 1:3 (AFZO75) and 0, 50 W for 0:1 (AZO). Single Al doped ZnO films (APZO series), in which AZO volume fraction was varied 0, 25, 50 and 75 % were also prepared by co-sputtering of pure ZnO and AZO targets, and their electrical and structural properties were compared with those of AFZO films. The sputter system was equipped with load-lock system, and the base pressure in the chamber was maintained below 5×10^{-7} Torr. Sputter deposition was carried out at working pressure of 1 mTorr using pure Ar gas and the substrate was not heated intentionally during the deposition. The distance between target and substrate also kept at 5 cm. For uniform deposition, the substrate was rotated with the controlled speed of 12 rpm. Annealing test of the deposited films was performed at the temperature of 300 ^{o}C for 2 hours inside the vacuum chamber pumped down to below 10^{-6} Torr. The electrical resistivity, Hall mobility and carrier concentration were determined from the Hall effect measurement equipment using van der Pauw method. For all the films, the thickness was kept at about 200 nm. The microstructures of films were analyzed using X-ray diffractometer (Rigaku). The optical transmittance and reflectance spectra were obtained on

UV/VIS spectrophotometer (Perkin Elmer Lambda 35) in the wavelength range from 250 to 1100 nm. For analysis of chemical binding energy of oxygen ions, XPS characterization was made for as-deposited and annealed films after surface pre-cleaning for 3 minutes.

3. Results and Discussion

3.1 Structural properties

The Figure 1(a) and 1(b) show the XRD profiles of the as-deposited and the vacuum annealed AFZO film series, respectively. All the as-deposited and the annealed films show strong (002) peaks of preferred orientation, together with relatively weak (101) and (103) peaks. It is notable that the intensity of (101) and (103) peaks for the as-deposited films slightly increased with increasing amount of AZO in the films, and that intensity of these peaks increased for the annealed films. It has been reported that (002) plane of ZnO had the lowest surface energy resulting in the preferred growth in (002) orientation at equilibrium growth condition while growth in other directions appearing at non-equilibrium growth condition such as low deposition temperature and high deposition rate [9]. No appreciable Al_2O_3 crystalline peak was found. Inactive Al atoms in the AZO films have been reported to be segregated into grain boundaries and to inhibit the crystallization and preferred orientation of ZnO [10].

In Figure 2(a), the full width at half maximum (FWHM) of (002) peaks obtained for AFZO series and APZO series samples are compared. For both AFZO and APZO film series, FWHM decreased with increasing AZO content, and vacuum annealing resulted in slight reduction of FWHM. These implies, following Scherrer formula [11], that the average crystallite size with (002) orientation increases with increasing Al content in the films, and that annealing causes an increase of the average crystallite size with (002) orientation. These observations imply that the addition of Al enhances crystal growth in ZnO films, while the crystal growth in the preferred orientation is inhibited. Figure 2(b) shows a plot of (002) peak

position with varying AZO content obtained for AFZO film series. The (002) peak position of all ZnO films were located at lower diffraction angle than the corresponding peak position of 34.47 ^{o} found in the bulk ZnO. This is consistent with the findings that as-deposited ZnO films at low substrate temperature usually had porous structures and tensile stresses in the direction of c-axis [9]. As can be seen from Figure 2(b), the annealing caused in the increase of (002) peak position for all the films, implying that the porous structure and the corresponding tensile stresses can be reduced by annealing. The diffraction peak position of (002) orientation shifts towards higher angle as AZO volume fraction increases, indicating that the lattice length in c-axis reduces with addition of Al to the films. This reduction in lattice length in c-axis with addition of Al to ZnO films is believed to stem from the ionic radii difference between Zn^{2+} (72 pm) and Al^{3+} (53 pm) [12]. It is notable that the peak position of the annealed AFZO75 and AZO films are almost similar. This indicates that Al dopants in ZnO films with above 75 % AZO volume fraction could not be incorporated into Zn sites and remained inactive. This is consistent with the result obtained from the measurement of the carrier concentration for AFZO75 and AZO films, in which they have similar carrier concentrations as shown in Figure 3.

3.2 Electrical properties

In Figure 3(a), 3(b) and 3(c), the carrier concentration, Hall mobility and the resistivity obtained for both AFZO and APZO series films before and after annealing are compared, respectively. The carriers of Al and F doped ZnO films are generated from both the intrinsic type of donors stemming from the interstitial Zn metals or the oxygen vacancies and the extrinsic type of donors stemming from the substitution of Al and F. By vacuum annealing the oxygen vacancies and the interstitial Zn metals can be created and the carrier concentration will increase [13]. After vacuum annealing the resistivity of all ZnO films became lowered

due to the increase of both carrier concentration and mobility. The minimum resistivity of 4.75×10^{-4} Ωcm could be obtained for AFZO50 films due to their high mobility and carrier concentration. Vacuum annealed AFZO25 film showed the maximum mobility of 42.2 cm^2/Vsec. Figure 4 shows the XPS oxygen 1s binding energy of as-deposited AZO, AFZO25, annealed AZO and AFZO25 films. The binding energy for O 1s of ZnO structure is 530 eV and that of Al_2O_3 is 531.6 eV. Chen et al. reported that the component of the O1s located at about 531.25 eV is attributed to O^{2-} ions in oxygen deficient regions [12]. The components of O 1s in Al_2O_3 and oxygen deficient regions can not be fitted clearly. The small O 1s component located at about 532 eV is mainly due to the chemisorbed oxygen impurities such as O^{2-}, O^- and O_2^-. ZnO thin films are chemically active and the oxygen will be adsorbed easily at the surface and grain boundary. These chemisorbed oxygen acts as trap site of free electrons and increase the potential barrier of grain boundary. Minami reported that the mobility of doped ZnO films with carrier concentrations of 10^{20} ~ 10^{21} cm^{-3} was mainly limited by the ionized impurity scattering, and ZnO films with carrier concentrations of 10^{19} ~ 10^{20} cm^{-3} was dominated by the grain boundary scattering [10]. Since all the films except pure ZnO film have carrier concentration in the range of 1×10^{20} ~ 5×10^{20} cm^{-3}, grain boundary scattering mechanism cannot be excluded completely. After vacuum annealing of AFZO25, the reduction of the high binding energy oxygen peak at about 532 eV can be seen clearly in figure 4(a), which implies that the grain boundary potential decreases due to the removal of the chemisorbed oxygen at the grain boundary. The annealed AZO film also showed the slight reduction of the high binding energy oxygen peak. It is notable from Figure 3 that vacuum annealing give rise to a pronounced increase in mobility while only a slight increase in carrier concentration is observed for all AFZO series films. This cannot be explained only by ionized impurity scattering because the mobility of highly degenerate semiconductor is known to be disproportional to carrier concentrations as $\mu \propto n^{-2/3}$ [14]. Although the average crystallite

size estimated from FWHM was all in the range of 30 ~ 40 nm and is larger than the electronic mean free path of all our ZnO films (below 6 nm), the grain boundary potential barrier is believed to influence the mobility of our ZnO films. The mobility decrease of AFZO films with the increase of AZO volume fraction might be explained by the ionized impurity scattering together with the grain boundary scattering. Upon comparing the electrical properties of APZO and AFZO series films, it is clear that vacuum annealing of APZO films also give rise to an increase of mobility but not as much as in the case of AFZO series films. Furthermore, the carrier concentration and the mobility of APZO series films lay below those of AFZO series films at the same volume fraction of AZO. Although Shanthi et al. reported that fluorine did not cause an increase in grain boundary potential in their F-doped tin oxide films [15], this could not be confirmed in our films. As shown in Figure 2, FWHM values of annealed APZO series films are lower than those of AFZO series films. This indicates that fluorine dopant promotes the crystallization of ZnO films and reduces grain boundary scattering, which eventually would lead to higher mobility observed in AFZO films.

3.3 Optical properties

Figure 5(a) and (b) show plots of the absorption coefficients obtained for the as-deposited and the annealed AFZO film series, respectively. The absorption coefficient was calculated from the measured optical transmittance and reflectance according to the following relation :

$$\alpha = \frac{1}{d}\ln\left(\frac{1-R}{T}\right) \qquad (1)$$

where T and R are the optical transmittance and reflectance of the films and d is the thickness of the films. High absorption in the short wavelength region is stemming from interband transition and the increase of absorption in the long wavelength region is due to free carrier absorption. By vacuum annealing, the absorption coefficients of all the films reduced for the most of visible and near IR range measured in this study. The decrease of absorption in the

short wave length region with annealing is due to the increase of the optical band gap according to Burstein-Moss effect. Figure 6 shows the optical band-gap energy (E_{opt}) determined by fitting the absorption coefficient data according to equation (2) derived for the direct band transition [16]:

$$(\alpha h\nu)^2 = A(h\nu - E_{opt}) \qquad (2)$$

where α is the absorption coefficient, ν is the photon frequency, and A is a constant. After vacuum annealing, the optical band gap of AFZO films all increased. Another possible reason is that voids between crystallites which scatter the light were reduced by annealing. The decrease of absorption coefficient in the long wavelength region for the vacuum annealed films is thought to be caused by the increase of mobility resulting from the low free carrier absorption. Free carrier absorption has been described by equation (2) following Drude model [16] :

$$\alpha = \frac{ne^3\lambda^2}{4\pi^2 c^3 N\mu\varepsilon_0 m^{*2}} \qquad (3)$$

where $n, \lambda, c, N, \varepsilon_0, m^*$ and μ are carrier concentration, wavelength, light speed, refractive index, vacuum permittivity, effective mass and mobility, respectively. The free carrier absorption is proportional to n/μ and the increase of mobility reduces the free carrier absorption. Good transparent and conducting oxides (TCOs) should have low resistivity and visible absorption. Quantitative measure of performance of transparent conducting oxide is figure of merit (FOM) defined as [13] :

$$\alpha = \frac{1}{\rho\alpha} \qquad (4)$$

Figure 7 shows a plot of FOM obtained for the as-deposited and the annealed AFZO film series. In this analysis, the absorption coefficient values averaged in the wavelength range from 400 to 800 nm were used. After annealing, FOM of all ZnO films increased noticeably

due to lower visible absorption and higher conductivity than before annealing. Annealed AFZO50 had the highest FOM value of 2.67 Ω^{-1}.

4. Conclusions

Transparent and conducting ZnO films doped with Al and F have been deposited on glass by co-sputtering ZnO:ZnF_2 and ZnO:Al_2O_3 ceramic targets. After annealing at 300 ^oC for 2 hours in vacuum, the minimum resistivity of 4.75×10^{-4} Ωcm was obtained for AFZO50 film, and the highest mobility of 42.2 cm^2/Vsec was found in AFZO25 thin film. From XRD measurements it was found that fluorine dopants enhanced the crystallization of ZnO and reduce grain boundary scattering. The analysis of XPS spectra for the as-deposited and the annealed AFZO25 films revealed that chemisorbed oxygen ions reduce the mobility of ZnO films, and that after vacuum annealing most of chemisorbed oxygen was removed giving in the increase in mobility. The highest optical bandgap energy of 3.8 eV was found in the annealed AZO film. Vacuum annealing of the AFZO films resulted in the decrease in both the optical absorption and the resistivity, giving the highest FOM of 2.67 Ω^{-1} for AFZO50 thin film. It can be concluded that dual doping of F and Al might be a plausible method for obtainment of transparent conducting ZnO films with higher performance.

References

[1] A. V. Singh, R. M. Mehra, N. Buthrath, A. Wakahara, and A. Yoshida., Higly conductive and transparent aluminum-doped zinc oxide thin films prepared by pulsed laser deposition in oxygen ambient, J. Appl. Phys., 2001, 90(11), 5661-5665.

[2] E. Fu, D. Zhuang, G. Zhang, Z. ming, W. Yang and J. Liu, Prperties of transparent conductive ZnO:Al thin films prepared by magnetron sputtering, Microelectronics J., 2004, 35, 383-387.

[3] K. Ellmer, Magnetron sputtering of transparent conductive zinc oxide: relation between the sputtering parameters and the electronic properties, J. Phys. D: Appl. Phys., 2000, 33, R17-R32.

[4] A. Sanchez-Juarez, A. Tiburcio-Silver and A. Oritz, Properties of fluorine-doped ZnO deposited onto glass by spray pyrolysis, Sol. Energy Mater. Solar Cells, 1998, 52, 301-311.

[5] S. Fujihara, J. Kusakado and T. Kimura, Fluorine doping in transparent conductive ZnO thin films by a sol-gel method using trifluoroacetic aced, J. Mat. Sci. Lett., 1998, 17, 781-783.

[6] M. Olvera, A. Maldonado and R. Asomoza, ZnO:F thin films deposited by chemical spray: effect of the fluorine concentration in the starting solution, Sol. Energy Mater. Solar Cells, 2002, 73, 425-433.

[7] J. Hu and R. Gordon, Textured fluorine-doped ZnO films by atmospheric pressure chemical vapor deposition and their use in amorphous silicon solar cells, Solar Cells, 1991, 30, 437-450.

[8] T. Minami, S. Ida, T. Miyata and Y. Minamino, Transparent conducting ZnO thin films deposited by vacuum arc plasma evaporation, Thin Solid Films, 2003, 445, 268-273.

[9] M. K. Puchert, P. Y. Timbrell, and R. N. Lamb, Postdeposition annealing of radio frequency magnetron sputtered ZnO films, J. Vac. Sci. Techno. A, 1996, 14(4), 2220-2230.

[10] T. Minami, H. Sato, K. Ohashi, T. Tomofuji and S. Takata, Conduction mechanism of highly conductive and transparent zinc oxide thin films prepared by magnetron sputtering, J. Cryst. Growth, 1992, 117, 370-374.

[11] B. D. Cullity, Elements of X-ray diffraction, Addison-Wesley Publishing Company, 1977, pp. 102.

[12] M. Chen, Z. L. Pei, C. Sun, L. S. Wen and X. Wang, Surface characterization of transparent conductive oxide Al-doped ZnO films, J. Cryst. Growth, 2000, 220, 254-262.

[13] G. J. Fang, D.J. Li and B.-L. Yao, Effect of vacuum annealing on the Properties of

tansparent conductive AZO thin films prepared by DC magnetron sputtering, Phys. Stat. Sol., 2002, 193(1), 139-152.

[14] M. Chen, Z. L. Pei, X. Wang, Y. H. Yu, C. Sun and L. S. Wen, J. Phys. D: Appl. Phys., 2000, 33, 2538-2548.

[15] E. Shanthi, A. Banerjee, V. Dutta and K. L. Chopra, Electrical and optical properties of tin oxide films doped with F and (Sb+F), J. Appl. Phys., 1982, 53(3), 1615-1621.

[16] D. Y. Young, Electron transport in zinc stannate (Zn2SnO4) thin films, Ph D theis, Colorado School of Mines, 2000.

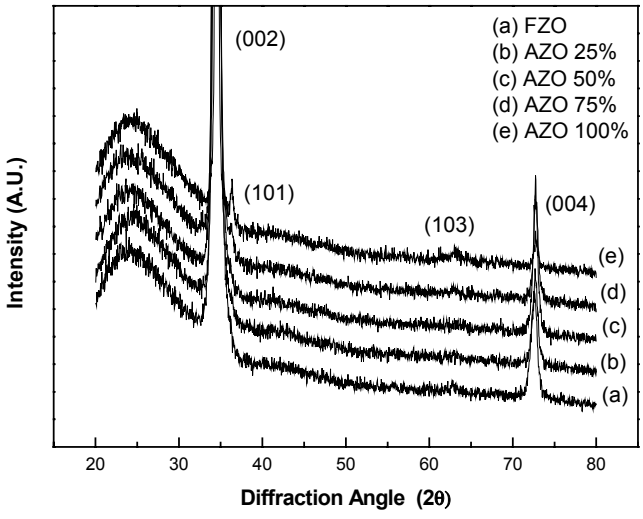

(a)

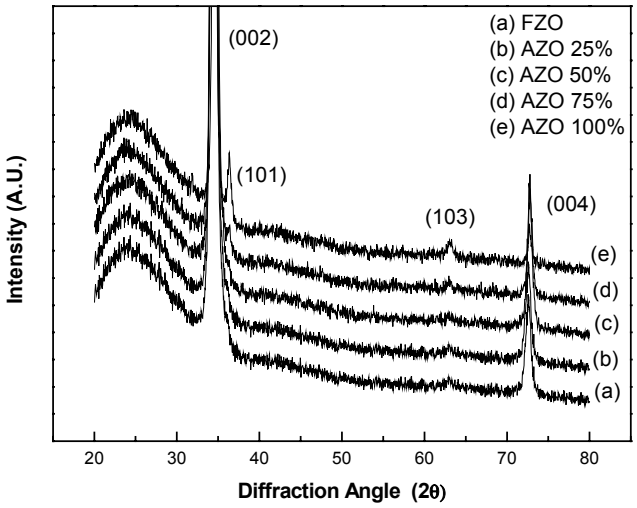
(a) FZO
(b) AZO 25%
(c) AZO 50%
(d) AZO 75%
(e) AZO 100%
(002)
(101)
(103)
(004)
(e)
(d)
(c)
(b)
(a)
Intensity (A.U.)
20
30
40
50
60
70
80
Diffraction Angle (2θ)

(b)

Figure 1

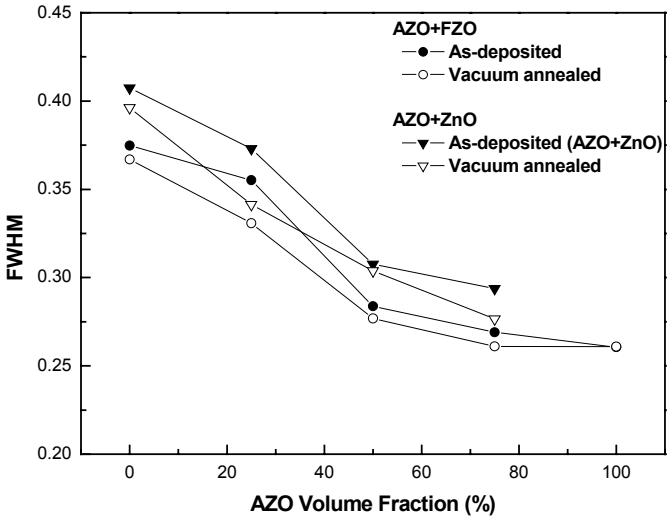
AZO+FZO
As-deposited
Vacuum annealed
AZO+ZnO
As-deposited (AZO+ZnO)
Vacuum annealed
FWHM
0.45
0.40
0.35
0.30
0.25
0.20
0
20
40
60
80
100
AZO Volume Fraction (%)

(a)

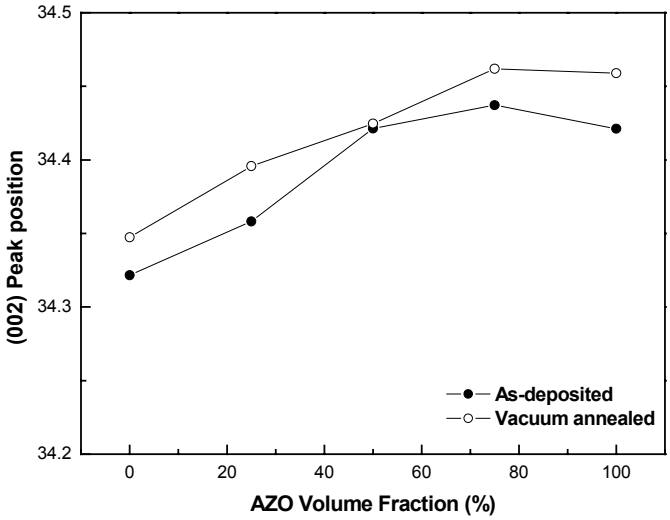
34.5
34.4
34.3
34.2
(002) Peak position
0
20
40
60
80
100
AZO Volume Fraction (%)
As-deposited
Vacuum annealed

(b)

Figure 2

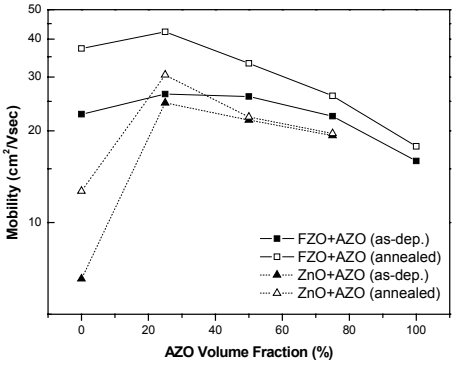
50
40
30
20
10
Mobility (cm²/Vsec)
0
20
40
60
80
100
AZO Volume Fraction (%)
FZO+AZO (as-dep.)
FZO+AZO (annealed)
ZnO+AZO (as-dep.)
ZnO+AZO (annealed)

(a)

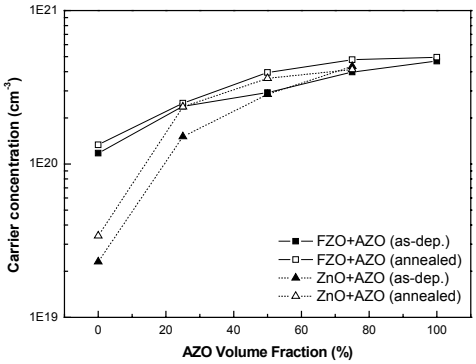
1E21
1E20
1E19
Carrier concentration (cm^{-3})
0
20
40
60
80
100
AZO Volume Fraction (%)
FZO+AZO (as-dep.)
FZO+AZO (annealed)
ZnO+AZO (as-dep.)
ZnO+AZO (annealed)

(b)

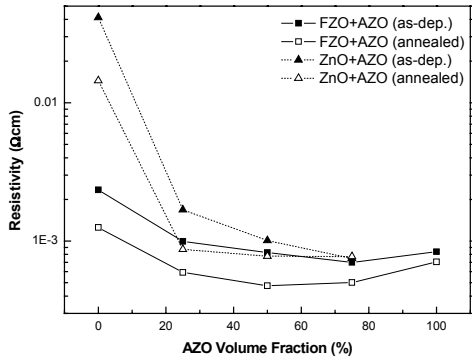
0.01
1E-3
Resistivity (Ωcm)
0
20
40
60
80
100
AZO Volume Fraction (%)
FZO+AZO (as-dep.)
FZO+AZO (annealed)
ZnO+AZO (as-dep.)
ZnO+AZO (annealed)

(c)

Figure 3

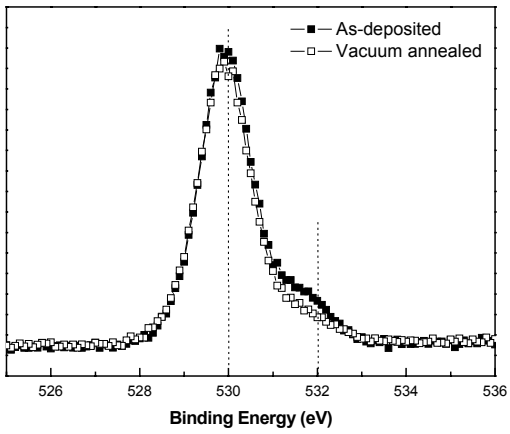
526
528
530
532
534
536
Binding Energy (eV)
As-deposited
Vacuum annealed

(a)

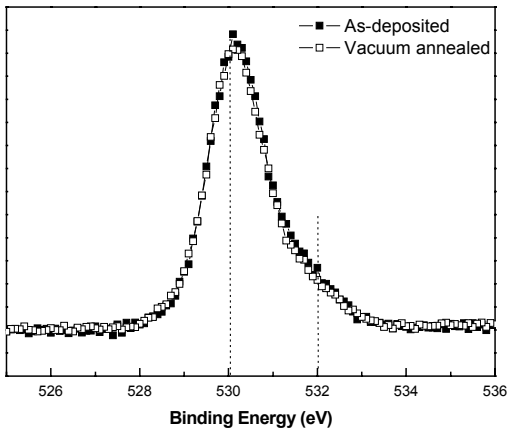
As-deposited
Vacuum annealed
526
528
530
532
534
536
Binding Energy (eV)

(b)

Figure 4

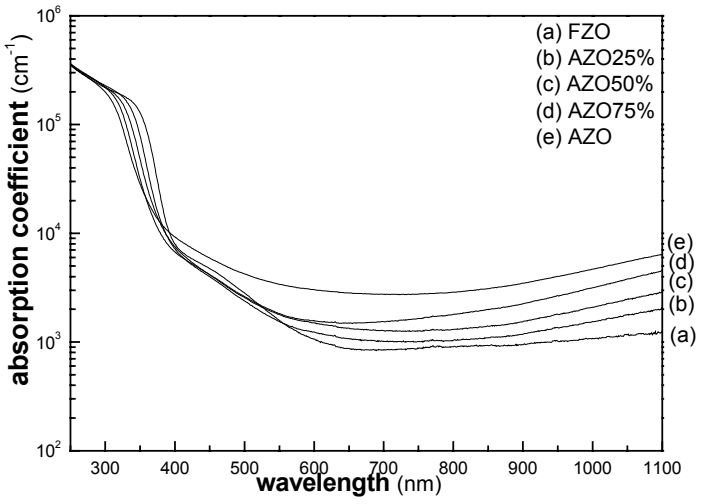
(a) FZO
(b) AZO25%
(c) AZO50%
(d) AZO75%
(e) AZO
absorption coefficient (cm-1)
wavelength (nm)
300
400
500
600
700
800
900
1000
1100
(e)
(d)
(c)
(b)
(a)

(a)

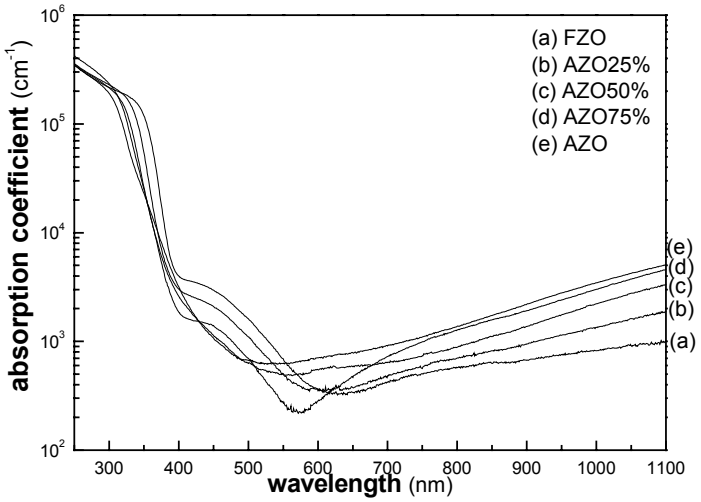
absorption coefficient (cm^{-1})
wavelength (nm)
(a) FZO
(b) AZO25%
(c) AZO50%
(d) AZO75%
(e) AZO
(e)
(d)
(c)
(b)
(a)

(b)

Figure 5

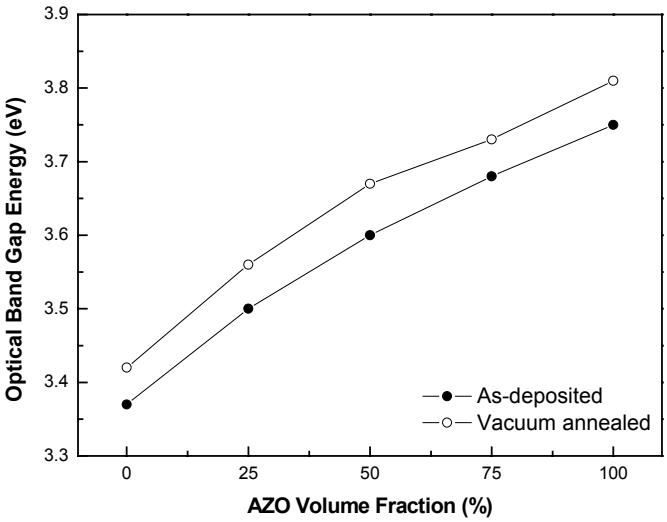
Optical Band Gap Energy (eV)
AZO Volume Fraction (%)
As-deposited
Vacuum annealed

Figure 6

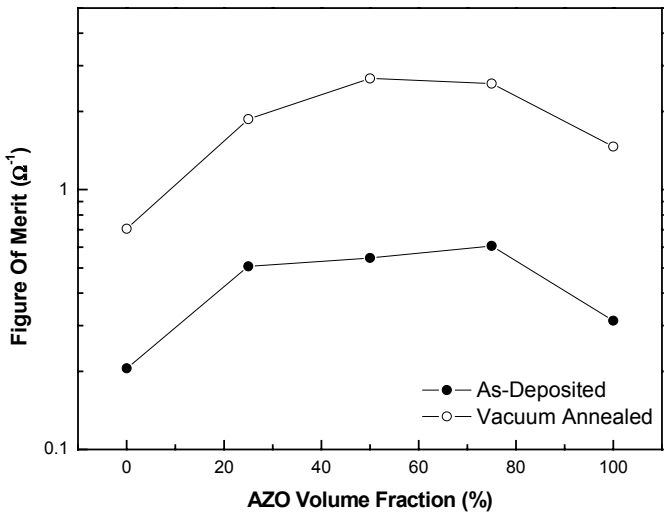
Figure Of Merit (Ω-1)
1
0.1
0
20
40
60
80
100
AZO Volume Fraction (%)
As-Deposited
Vacuum Annealed

Figure 7

List of Fiqures